Journal of Applied Science and Engineering, Vol. 22, No. 2, pp. 273–287 (2019) *DOI: 10.6180/jase.201906_22(2).0009*

Integrating SINS Sensors with Odometer Measurements for Land Vehicle Navigation System

Susu Fang, Zengcai Wang* and Jiacheng Fan[3]

Key Laboratory of High-efficiency and Clean Mechanical Manufacture, Ministry of Education, College of Mechanical Engineering, Shandong University, Jinan, P.R. China

Abstract

This paper details a new model for land vehicle navigation including attitude, velocity, and position estimation using an odometer (OD) and a magnetometer (MAG) in conjunction with strapdown inertial navigation system (SINS) sensors. In this new model, the SINS/OD navigation system is designed firstly. In SINS/OD system, the application of non-holonomic constraints for obtaining virtual velocity measurements is investigated and an innovation-based estimation adaptive (IAE) Kalman filter is designed to provide a land vehicle navigation solution by combining the velocity measurement from an odometer and error in the centripetal acceleration difference as a new observable from SINS sensors. In addition, an adaptive federated Kalman filter (AFKF) is designed, which integrates the magnetometer on the basis of the SINS/OD navigation system. It is shown that the accuracy of the new method is higher than of SINS, and using it with the magnetometer in the integrated navigation system yields more accurate estimations. Finally, field tests show that the SINS/OD/MAG system improves the precision of the navigation system and promotes a fault-tolerant performance. The proposed approach can be used as a backup navigation system during outages of the Global Positioning System (GPS) for an extended amount of time with the navigation error noticeably bounded. The redundancy and integrity of the entire navigation system are also further enhanced.

Key Words: Navigation System Model, Vehicle Integrating Navigation, Kalman Filter, Fault-tolerant performance

1. Introduction

In recent years, the research on the micro electro-mechanical systems (MEMS)-based inertial measurement unit (IMU) has undergone rapid development, which has led to the use of strapdown inertial navigation systems (SINS) in the field of civil navigation. The main advantages of MEMS are their small size, light weight, better rigidity, higher resonant frequency, and wider bandwidth than large components [1]. However, SINS has a disadvantage that its navigation errors get accumulated in a short time, so that such devices do not satisfy the long-time, high-precision navigation requirements of land vehicles. Therefore, under the existing conditions, SINS is generally not used alone but combined with other navigation devices to form a joint navigation system [2].

Vehicle dead reckoning (DR) system is a commonly used autonomous vehicle positioning system. Generally, DR is combined with the Global Positioning System (GPS) and map matching (MM) to form a GPS/DR, MM/DR, or GPS/MM/DR integrated navigation system. It has the advantages of lower cost, higher precision, and better reliability. Concurrently, an inertial navigation system (INS) is also a DR model. Its errors accumulate over time so that SINS needs to be combined with the GPS and other navigation sensors [3]. Because SINS can offer larger number of precise navigation parameters

*Corresponding author. E-mail: wangzc@sdu.edu.cn

than a DR, which can improve the accuracy if it combinate with the GPS. And the efficiency can be promoted when match a map. However, because the GPS has the disadvantages of a multi-path transmission error and sensitivity of the signal to building occlusion, the performance of the vehicle navigation and positioning system after combination is significantly affected. So it is very meaningful to propose an approach can be used as a backup navigation system during outages of the Global Positioning System (GPS) for an extended amount of time with the navigation error noticeably bounded.

Odometer (OD) is a widely used positioning method. It records the motion of a carrier via an optical encoder mounted on the wheel, thereby calculating the position and speed of the carrier. Among them, the doppler velocity log (DVL) is completely independent of the limitations of the external environment, and it has a fast response speed and good concealment. It is also widely used in integrated navigation systems [4]. Benchuan Zhou et al. combined SINS, the GPS, and DVL sensors to improve the accuracy of the entire integrated navigation system using a federal Kalman filter [5]. At present, integrated navigation is the main mode of vehicle autonomous navigation. The research on vehicle integrated navigation solutions nationally and internationally includes GPS/DR, GPS/MM, GPS/DR/MM, GPS/SINS, and SINS/OD [6]. In these vehicle integrated navigation solutions, some of them use GPS except for SINS/OD, which are still no way to avoid the disadvantage of GPS signal loss [7].

In many applications, gyroscopes have been successfully used to determine the attitude of the system. However, for long-duration working systems, gyroscope drift errors can lead to inaccurate attitudes. With low-cost gyroscopes, such as MEMS gyroscopes, the drift error can reach insignificant levels within tens of seconds [8]. In addition to using gyroscopes, accelerometers and magnetometers can also be used to obtain attitude angles. The attitude determined by an accelerometer and MAG does not drift, but the accuracy of the combination is affected by the accuracy of the sensor itself. Therefore, in the application of the attitude and heading reference system (AHRS), the combination of a gyroscope, an accelerometer, and magnetometer is used to obtain the navigation attitude in a complex scenario [9]. In an inertial navigation system, a magnetometer can be used for initial alignment or as a measurement vector to suppress the gyroscope drift [10]. The application of MAG has become an important research direction for integrated navigation systems [11,12]. Thus, the article proposed SINS/OD/MAG navigation system has the advantages of complementary advantages and avoidance of weaknesses.

In integrated navigation, the earlier Kalman filter has undergone a series of improvements. The initially proposed Kalman filter theory is only applicable to a stochastic linear Gaussian system in which both the equation of state and measurement equation are all linear. For more than ten years later, Bucy and Sunahara and others were committed to the research on extending the classical Kalman theory for the estimation of nonlinear stochastic system [13] filtering, and they proposed the extended Kalman filter (EKF) theory for discrete nonlinear stochastic systems [14]. Because the computational complexity of a Kalman filter increases dramatically with the cube of the state dimension, a centralized Kalman filter often fails to meet the real-time requirements for high-dimensional systems and has the disadvantage of poor fault tolerance [15]. Since 1988, Carlson has proposed federated filtering based on this theory, aiming to propose a method for the design of fault-tolerant integrated navigation systems. A federal filter adopts the design concept of decentralized filtering followed by global fusion, which significantly improves the fault tolerance of the system. The United States Air Force has now identified the federal filter as a universal filter for the new generation of navigation systems.

This paper proposes an integrated navigation system integrating the odometer and magnetometer information in an inertial navigation system. Firstly, the SINS/odometer integrated navigation system is designed, and then the innovation-based estimation adaptive Kalman filter (AKF) is used to estimate the system and measurement noise to improve the system fault-tolerance performance. Non-holonomic constraints are applied to obtain the virtual velocity measurements, and the centripetal acceleration closing difference is employed as one of the observations to obtain better navigation results. On this basis, a SINS/MAG integrated navigation system is added, and in the former, an accelerometer and MAG are used to determine the attitude angle for ensuring the accuracy of

the yaw angle estimation. The federated Kalman filter is used to fuse the two local systems, whereas INS is used as a public reference system. An adaptive allocation of the public reference information is implemented during the FKF innovation process, which improves the system fault tolerance and reliability.

The structure of the remaining paper is organized as follows: in the second part, the measurement of the view measurement of the SINS/odometer integrated navigation system is performed. The innovation-based estimation AKF algorithm is described in part three. The fourth part introduces SINS as a public reference system, where an odometer and a MAG are used as subsystems in the FKF. The fifth part presents the comparative analysis of an actual vehicle experiment and the experimental results of both integrated navigation systems. Finally, the conclusion is presented.

2. Measurement Equation of SINS/OD

2.1 Non-holonomic Constraints

We discuss a general vehicle movement in the two-dimensional space. The carrier coordinate and navigation coordinate systems are set as shown in Figure 1. The origin of the carrier coordinate system (frame *b*) is located at the centre of the mass of the vehicle. The *x* axis is parallel to the vehicle front and rear wheel axles and points to the right side of the vehicle. The *y* axis points to the forward direction of the vehicle, and the z axis is perpendicular to the *x* axis, and the y axis points above the vehicle. The local geographic frame, east-north-up (ENU) is selected as the navigation frame, located exactly at the centre of the vehicle (frame *n*).

During the movement of a vehicle, we can assume that the vehicle does not slip and will not leave the ground, i.e. the *x* and *z* axis speeds of the vehicle are not sufficiently close to zero in the carrier coordinate system. Then from the non-holonomic constraints of the vehicle movement we can obtain

$$v_x^b - \upsilon_x = 0 \tag{1}$$

$$v_z^b - \upsilon_z = 0 \tag{2}$$

where v_x^b and v_z^b are the speed components in the *x* and *z* directions in the carrier coordinate system, respectively. υ_x and υ_z are Gaussian white noises, both of whose means are zero, and the variances are σ_x^2 and σ_z^2, respectively. Another speed measured by the odometer is v_y^b. Therefore, we can obtain v_{od}^b, which is the speed measured by the odometer in the carrier coordinate system:

$$v_{od}^b = [v_x^b \quad v_y^b \quad v_z^b]^T \tag{3}$$

When it is converted to the navigation coordinate system, it is expressed as

$$v_{od}^n = \boldsymbol{C}_b^n * \begin{bmatrix} v_x^b \\ v_y^b \\ v_z^b \end{bmatrix} \tag{4}$$

Among these parameters, v_{od}^n is the speed measured by the odometer under the non-holonomic constraint in the navigation coordinate system. C_b^n is the attitude direction cosine matrix (DCM) from frame *b* to frame *n*, which is often used to transform the specific force to the navigation coordinate frame.

The attitude matrix can be obtained by the Euler angle method. The conversion process from frame *b* to frame *n* is as follows: The navigation coordinate system (frame *n*) is rotated by angle ψ around the z-axis to obtain coordinate system n_1. The n_1 coordinate system is rotated by angle ξ around the y-axis to obtain the n_2 coordinate system, and the n_2 coordinate system is rotated by angle ϑ around the x-axis to obtain frame *b*. Therefore, the Euler angle can be used to obtain attitude matrix C_n^b

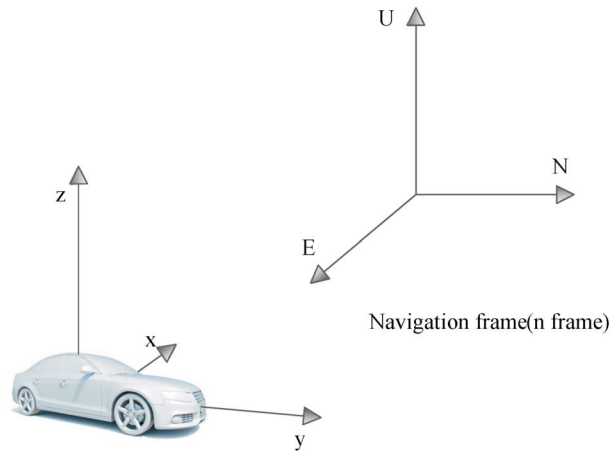

Figure 1. Schematic of the frame coordinates.

from frame *n* to frame *b* as follows:

$$\boldsymbol{C}_n^b = \boldsymbol{C}_{n_2}^b \boldsymbol{C}_{n_1}^{n_2} \boldsymbol{C}_n^{n_1} \tag{5}$$

Transposing C_n^b yields C_b^n, which is expressed as follows:

$$\boldsymbol{C}_b^n = \begin{bmatrix} \cos\xi\cos\psi & -\cos\vartheta\sin\psi+\sin\vartheta\sin\xi\cos\psi & \sin\vartheta\sin\psi+\cos\vartheta\sin\xi\cos\psi \\ \cos\xi\sin\psi & \cos\vartheta\cos\psi+\sin\vartheta\sin\xi\sin\psi & -\sin\vartheta\cos\psi+\cos\vartheta\sin\xi\sin\psi \\ -\sin\xi & \sin\vartheta\cos\xi & \cos\vartheta\cos\xi \end{bmatrix} \tag{6}$$

where ϑ, ξ, and ψ, respectively, represent the pitch angle, roll angle, and yaw angle in the attitude angle of the inertial navigation system.

2.2 Centripetal Acceleration Observation

In general, most vehicles are front-wheel steering vehicles. When a vehicle is steering, its instantaneous movement can be seen as a circular movement centred on a point on the extension line of the longitudinal axis of the vehicle. When the vehicle is traveling in a straight line, the vehicle motion can also be regarded as a circular motion with an infinite radius of curvature [16]. As shown in Figure 2, point O is the centre of the circular motion and is located on the x-axis of the vehicle coordinate system.

For using calculus to analyse the circular motion, the vehicle is supposed to move from point *A* to point A_1 in a very short time. The moving distance is *dl*, and angle of the change in the speed direction is *d*φ. As shown in the following figure, we can obtain instantaneous radius of curvature ρ during the motion of the vehicle, as follows:

$$\rho = v_y^b / \dot{\phi} \tag{7}$$

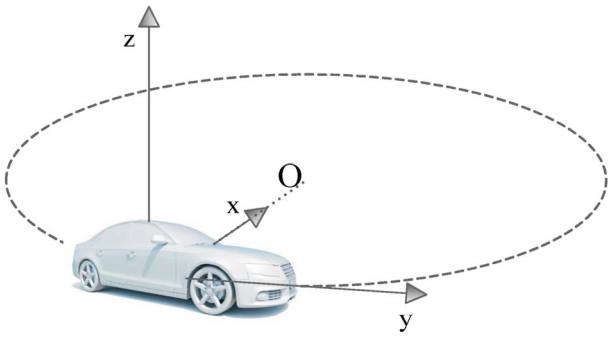

Figure 2. Schematic of the vehicle circular motion.

where the velocity in the y-axis direction in the carrier coordinate system is v_y^b and the angular velocity around the axis of the vehicle carrier coordinate system is $\dot{\phi}$, and the point o is the centre of the circular motion in Figure 3.

According to the principle of circular motion, the expression for centripetal acceleration a_x can be derived as

$$a_x = (v_y^b)^2 / \rho = v_y^b \dot{\phi} \tag{8}$$

Set *D* as the centripetal acceleration difference, which can be expressed as:

$$D = a_x - v_y^b \dot{\phi} \tag{9}$$

and

$$D = 0 \tag{10}$$

The centripetal acceleration, y-axis velocity of the carrier coordinate system, and angular velocity around the y-axis can be measured and calculated by inertial navigation system as shown in the following equations:

$$\tilde{a}_x = f_x^b + (C_n^b g^n)_x \tag{11}$$

$$\tilde{v}_y^b = (\tilde{\boldsymbol{C}}_n^b \tilde{v}^n)_y \tag{12}$$

$$\tilde{\dot{\phi}} = \omega_{nbz}^b \tag{13}$$

Because the angular velocity of the rotation of the earth and rotational angular velocity of the vehicle which relative to the earth are extremely minuteness, they can be written as

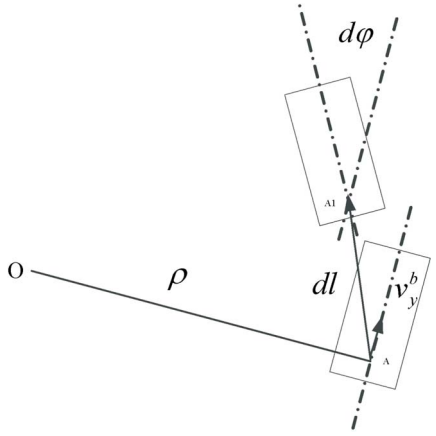

Figure 3. Schematic of the vehicle circular motion.

$$\begin{aligned}\omega_{nbz}^{b} &= \omega_{ibz}^{b} - \omega_{inz}^{b} = \omega_{ibz}^{b} - (C_n^b \omega_{in}^n)_z \\ &= \omega_{ibz}^{b} - (C_n^b(\omega_{ie}^n + \omega_{en}^n))_z \\ &\approx \omega_{ibz}^{b}\end{aligned} \tag{14}$$

Therefore, equation (15) can be simplified as

$$\tilde{\dot{\phi}} \approx \omega_{ibz}^{b} \tag{15}$$

In the above equations, $\tilde{a}_x$, $\tilde{v}_y^b$, and $\tilde{\varphi}$ are the observations of a_x, v_y^b, and $\dot{\varphi}$, respectively; f_x^b is the x-axis acceleration in the carrier coordinate system measured by an accelerometer; g^n is the gravitational acceleration in the navigation coordinate system; i, e, n, and b represent the inertial coordinate system, geocentric coordinate system, navigation coordinate system, and carrier coordinate system, respectively; ω_{nb}, ω_{ib}, ω_{in}, ω_{ie}, and ω_{en} indicate the rotational angular velocity vector of frame b relative to frame n, frame b relative to frame i, frame n relative to frame i, frame e relative to frame i, and frame n relative to frame e, respectively. Superscripts n and b represent the decomposition of the corresponding values in frame n and frame b, respectively, and z as a subscript indicates the z-axis direction.

The observation of D can be represented as

$$\tilde{D} = \tilde{a}_x - \tilde{v}_y^b \tilde{\dot{\phi}} \tag{16}$$

In summary, the error in the centripetal acceleration difference can be taken for SINS/OD as another observation,

$$\begin{aligned}z_{ac} &= \tilde{D} - D = \tilde{a}_x - \tilde{v}_y^b \tilde{\dot{\phi}} \\ &= f_x^b + (C_n^b g^n)_x - (\tilde{C}_n^b \tilde{v}^n)_y \omega_{ibz}^b\end{aligned} \tag{17}$$

3. Adaptive Kalman Filter

3.1 System Observation Model

Before designing the Kalman process model, the error state model should be defined. Typically, the SINS error model is defined in the navigation frame system. The error propagation equations for the attitude velocity and position in the navigation frame system can be expressed by the following equations:

$$\dot{\phi}^n = -\left(\omega_{ie}^n + \omega_{en}^n\right) \times \phi^n + \delta\omega_{ie}^n + \delta\omega_{en}^n + C_b^n \varepsilon_g^b \tag{18}$$

$$\begin{aligned}\delta\dot{v}^n = &\left(C_b^n f^b\right) \times \phi^n - \left(2\delta\omega_{ie}^n + \delta\omega_{en}^n\right) \times v^n \\ &- \left(2\omega_{ie}^n + \omega_{en}^n\right) \times \delta v^n + C_b^n \varepsilon_a^b\end{aligned} \tag{19}$$

$$\delta\dot{\boldsymbol{P}} = \delta\varsigma \boldsymbol{v}^{\mathrm{n}} + \varsigma\delta\boldsymbol{v}^{\mathrm{n}} \tag{20}$$

where ϕ^n is the attitude angle error in the navigation frame, δ is the error of the corresponding physical quantity, and δv^n δP are the speed and position errors, respectively. ε_g and ε_a are the gyroscope and accelerometer measurement errors, respectively. ς is the transformation matrix from the vehicle velocity to the angular.

From the above equations, a sixteen-dimension state vector can be obtained to estimate the biases of the gyroscopes, accelerometers and the error in the scale factor. It is

$$X = \begin{bmatrix} \phi^{nT} & \delta v^{nT} & \delta P^T & \varepsilon_g^{bT} & \varepsilon_a^{bT} & \delta K \end{bmatrix}^T \tag{21}$$

where δK is the scale factor of the odometer which contains both the constant and random errors [17]. The accelerometer, gyroscope, and odometer measurement errors can be considered constant over a short time. Therefore, ε_g, ε_a, and δK satisfy the following equations:

$$\dot{\varepsilon}_g = 0 \tag{22}$$

$$\dot{\varepsilon}_a = 0 \tag{23}$$

$$\delta K = 0 \tag{24}$$

Finally, the error model is defined as

$$\dot{X} = F_{SINS} X + w \tag{25}$$

F_{SINS} is the 16 × 16 dimensional state transition matrix of SINS [18] and w is the system noise vector.

Based on the speed measured by the odometer in the navigation coordinate system under the non-holonomic constraint, v_{od}^n, and considering the attitude error and scale factor error, we can obtain the odometer observation in frame n.

$$\begin{aligned}\tilde{v}_{od}^n &= [I_{3\times3} - (\phi\times)] C_b^n (1 + \delta K) v_{od}^b \\ &= v_{od}^n + \delta K v_{od}^n + v_{od}^n \times \phi - \delta K v_{od}^n \times \phi\end{aligned} \tag{26}$$

where ϕ is the attitude angle error, and $\phi\times$ is the skew-

symmetric matrix of ϕ.

Simplifying the above equation:

$$\tilde{v}_{od}^{n} = v_{od}^{n} + \delta K v_{od}^{n} + v_{od}^{n} \times \phi \tag{27}$$

Therefore, the error in the difference between the odometer measurement and observation can be written as

$$\delta v_{od}^{n} = \tilde{v}_{od}^{n} - v_{od}^{n} = \delta K v_{od}^{n} + v_{od}^{n} \times \phi \tag{28}$$

Considering SINS velocity error δv_{SINS}^{n} in frame n, the velocity residual can be obtained as

$$z_{v} = \delta v_{SINS}^{n} - \delta K v_{od}^{n} - v_{od}^{n} \times \phi \tag{29}$$

Thus, with equations (17) and (29), the measurement vector can be expressed as

$$Z_k = [z_v \quad z_{ac}]^T \tag{30}$$

Then, the measurement equation is given as

$$Z_k = H_k X + v \tag{31}$$

where $X = [\phi^{nT} \quad \delta v^{nT} \quad \delta P^{T} \quad \varepsilon_{g}^{bT} \quad \varepsilon_{a}^{bT} \quad \delta K]^T$, $H_k = [H \quad M]^T$, $H = \begin{bmatrix} 1 & 0 & 0 & 0 & -v_{odU}^{n} & -v_{odN}^{n} & 0_{1\times 9} & -v_{odE}^{n} \\ 1 & 0 & 0 & v_{odU}^{n} & 0 & -v_{odE}^{n} & 0_{1\times 9} & -v_{odN}^{n} \end{bmatrix}$, $M(1,1) = C_b^n(1,2)g_0 - C_b^n(2,3)v_y^n - C_b^n(2,2)v_y^n\omega_{ibz}^b$, $M(1,2) = -C_b^n(1,1)g_0 - C_b^n(2,1)v_z^n - C_b^n(2,3)v_x^n\omega_{ibz}^b$, $M(1,3) = -(C_b^n(2,2)v_x^n - C_b^n(2,1)v_y^n)\omega_{ibz}^b$, $M(1,4) = -C_b^n(2,1)\omega_{ibz}^b$, $M(1,5) = -C_b^n(2,2)\omega_{ibz}^b$, $M(1,6) = -C_b^n(2,3)\omega_{ibz}^b$, $M(1,13) = 1$, $M(1,12) = -C_b^n(2,1)v_x^n - C_b^n(2,2)v_y^n - C_b^n(2,3)v_z^n$, where the remaining elements of matrix M are 0. H is the observation matrix, and E, N, U are represents east, north, and up directions respectively. v is the observation noise vector, which is assumed to be a Gaussian white noise.

The system state model is established as depicted in Figure 4. Then the state can be estimated according to the Kalman filtered inference algorithm.

3.2 Measurements Fusion Using AKF

It is known that it is difficult to obtain the accurate noise density without the precise knowledge of the model and noise characteristics. In conventional Kalman filters, measurement noise covariance matrix R and process noise covariance matrix Q are fixed and known a priori. Therefore, we have applied the innovation-based estimation adaptive (IAE) Kalman filter method to automatically tune the measurement noise covariance [19]. The IAE Kalman filter is a method that adjusts the Kalman gain matrix online by estimating the innovation sequence. The brief structure of the integrated system is shown Figure 5. This method directly corrects the Kalman filter gain by measuring the actual innovation sequence and improves the accuracy and robustness of the attitude, velocity, and position for vehicle navigation.

The state equation and measurement equation of a discrete linear system model are as follows:

$$\begin{cases} X_k = \Phi_{k,k-1} X_{k-1} + \Gamma_{k-1} W_{k-1} \\ Z_k = H_k X_k + V_k \end{cases} \tag{32}$$

where $\Phi_{k,k-1}$ is the state transition matrix, Γ_{k-1} is the system noise drive matrix, and W_{k-1} and V_k are the independent Gaussian white noise with zero mean, respec-

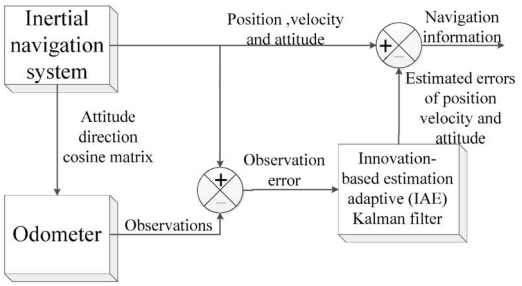

Figure 4. SINS/OD integrated navigation system.

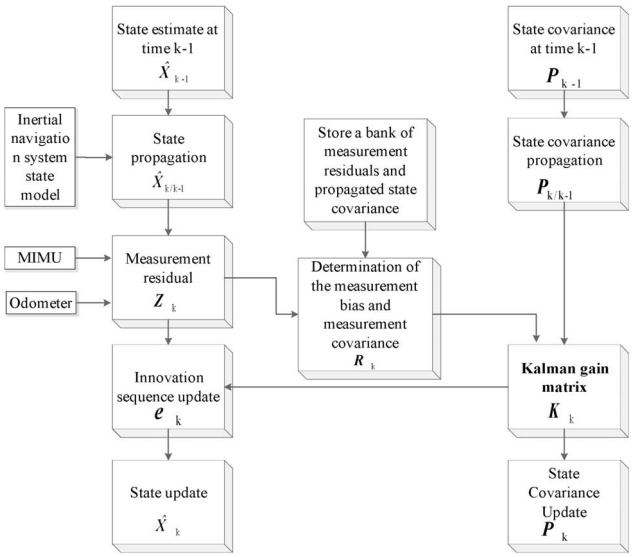

Figure 5. Flow chart of the innovation-based estimation adaptive (IAE) Kalman filter.

tively. They are shown as $W_k \sim N(0, Q)$; $V_k \sim N(0, R)$.

Considering innovation sequence e_k, the standard Kalman filter algorithm [20] can be obtained as follows:

$$\hat{X}_{k/k-1} = \Phi_{k,k-1}\hat{X}_{k-1} \tag{33}$$

$$P_{k/k-1} = \Phi_{k,k-1}P_{k-1}\Phi_{k,k-1}^T + \Gamma_{k-1}Q_{k-1}\Gamma_{k-1}^T \tag{34}$$

$$\hat{X}_k = \hat{X}_{k/k-1} + K_k e_k \tag{35}$$

$$K_k = P_{k/k-1}H_k^T\left(H_k P_{k/k-1}H_k^T + R_k\right)^{-1} \tag{36}$$

$$P_k = \left(I - K_k H_k\right)P_{k/k-1}\left(I - K_k H_k\right)^T + K_k R_k K_k^T \tag{37}$$

where e_k is the innovation sequence and e_k is the variance of the innovation sequence.

$$e_k = Z_k - H_k\hat{X}_{k/k-1} \tag{38}$$

$$C_{vk} = H_k P_{k/k-1}H_k^T + R_k \tag{39}$$

Assuming Q_k is stable, V_k is the independent Gaussian white noise with zero mean, and its variance R_k segment changes with time. The intensities of the noise changes in each segment are unknown and not related to each other, so that we can get

$$R_k^* = \frac{1}{N}\sum_{k-N+1}^{k} e_k e_k^T \tag{40}$$

where N is the number of samples and R_k^* is the measurement noise covariance matrix estimated online. Replacing R_k with R_k^* in equations (36) and (37), the innovation-based estimation adaptive Kalman filter algorithm can be designed.

4. SINS/OD/MAG System Model

4.1 SINS/MAG Error State Model

The federated Kalman filter is a distinct form of the distributed Kalman filter. The particularity of this filtering method lies in its unique information distribution principle and global optimum estimation method. Therefore, we design the SINS/MAG navigation system as another local filter, which based on the SINS/odometer navigation system and acting as the local filter. Similar to the AHRS system, SINS and MAG can form a local filter to improve the accuracy of the integrated navigation system attitude.

The fifteen-dimension state vector of this local filter is like that of the SINS/OD local filter

$$X = \left[\phi^{nT} \quad \delta v^{nT} \quad \delta P^T \quad \varepsilon_g^{bT} \quad \varepsilon_a^{bT}\right]^T \tag{41}$$

When the system is static, the gravitational component in frame n can be expressed as

$$f^n = [0 \;\; 0 \;\; -g_0]^T \tag{42}$$

Considering the misalignment angle error, the gravitational component in frame n, which is measured by an accelerometer, can be expressed as

$$f^{n_c} = \left(I - \phi\times\right)C_b^n f^b \tag{43}$$

Residual δf between f^n and f^{n_c} is considered as the observation of the local filter, where g_0 is the local gravitational acceleration.

$$\begin{bmatrix}\delta f_E\\ \delta f_N\\ \delta f_U\end{bmatrix} = \begin{bmatrix}-g_0 & 0 & 0\\ 0 & g_0 & 0\\ 0 & 0 & 0\end{bmatrix}\begin{bmatrix}\phi_E\\ \phi_N\\ \phi_U\end{bmatrix} \tag{44}$$

In inertial navigation system, initial alignment is needed before integral operation. The purpose of initial alignment is that the initial attitude angle is adjusted to a certain precision attitude as soon as possible. Initial alignment is the process of determining the direction between the axis of the inertial navigation system and the axis of the coordinate system. Due to the poor accuracy of gyroscope, the azimuth self-alignment can't be completed. Therefore, the magnetometer is combined with accelerometer in MIMU to determine attitude and accomplish initial alignment of inertial navigation system. During the initial alignment process, accelerometers and magnetometers are used to determine the attitude and obtain the accuracy of the yaw angle. When system is stationary, the direction of the gravity and local magnetic field can be used to stabilize the roll angle and pitch angle. When the pitch angle and roll angle is known, the yaw angle can be determined by magnetometer according to the geometrical relationship. When the vehicle is

still at a stationary state or at a constant velocity movement state, the accelerometer can measure the gravity component in the vehicle coordinate system precisely. In dynamic process, if the pitch and roll angle converge to a certain precision, the yaw angle can be derived as [21]:

$$\psi_c = -\tan^{-1}\left(\frac{m_y \sin\xi\cos\vartheta - m_z \sin\vartheta}{m_x \cos\xi + m_y \sin\vartheta\sin\xi + m_z \cos\vartheta\cos\xi}\right)$$

where m_x, m_y and m_z are the geomagnetic vector measured in the body frame. Therefore, heading residual Z_ψ between the magnetometer and gyroscopes is obtained as another observation; it can be expressed as

$$z_\psi = \tilde{\psi}_{sins} - \psi_{mag} = y + \delta\psi_{mag} \tag{45}$$

In the above equation, the value of $\delta\psi_{mag}$ depends on the latitude and longitude. However, during the driving process, the values of the latitude and longitude change by only small amounts, which we can ignore. ψ is the final residual, which is the azimuth error of the SINS. $Z_{2,k}$ can be expressed as

$$Z_{2,k} = [\delta f \;\; z_\psi]^T \tag{46}$$

The measurement equation is obtained as

$$Z_{2,k} = H_{2,k}X_2 + v_{2,k} \tag{47}$$

where $H_{2,k} = \begin{bmatrix} 0 & & -g_0 & 0 & 0 \\ 0_{3\times5} & 0 & 0_{3\times6} & 0 & g_0 & 0 \\ & 1 & & 0 & 0 & 1 \end{bmatrix}$ and $v_{2,k}$ is the observation noise vector, which is assumed to be a Gaussian white noise.

4.2 Federated Kalman Filter

This federated Kalman filter algorithm estimates the error by observing the vector and error model in the local filter to obtain the local optimum estimate. After this step, the local optimum estimation information of each local filter is fused to obtain the global optimum estimate such that the attitude, speed, and position error can be constantly revised during the updating process. The structure of the SINS/OD/MAG navigation system is illustrated in Figure 6; it uses SINS as the reference system, odometer as subsystem 1, SINS/OD as local filter 1, MAG as subsystem 2, and SINS/MAG as local filter 2. SINS output X_k is used to update the state quantities in the main filter and two local filters (partial filters) as the measured values. The output of each subsystem serves as the input for the corresponding local filter. Local optimum estimate of each local filter $\hat{X}_i$ and its covariance matrix P_i are fused in the main filter to obtain the global optimum estimate and corresponding covariance matrix.

The system states of the two subsystems are expressed respectively as

$$\begin{cases} X_{i,k} = \Phi_{i,(k,k-1)}X_{i,k-1} + \Gamma_{i,k-1}W_{i,k-1} \\ Z_{i,k} = H_{i,k}X_{i,k} + V_{i,k} \end{cases}, \; i = 1,2 \tag{48}$$

When $i = 1$, the system states express the SINS/OD system, and $X_{1,k}$, $Z_{1,k}$, $H_{1,k}$, $\Gamma_{1,k-1}$, $W_{1,k}$, and $V_{1,k}$ are equal to X_k, Z_k, H_k, Γ_{k-1}, W_k, and V_k in the SINS/OD system, respectively, when $i = 2$, the system states express the SINS/MAG system, and $X_{2,k}$, $Z_{2,k}$, $H_{2,k}$, $\Gamma_{2,k-1}$, $W_{2,k}$, and $V_{2,k}$ are as obtained in the previous section.

Each local filter independently utilizes the measurement information of the corresponding sensor for measurement and updating; the updating process is as follows:

$$\hat{X}_{i,k} = \hat{X}_{i,k/k-1} + K_{i,k}(Z_{i,k} - H_{i,k}\hat{X}_{i,k/k-1}) \tag{49}$$

$$K_{i,k} = P_{i,k/k-1}H_{i,k}^T\left(H_{i,k}P_{i,k/k-1}H_{i,k}^T + R_{i,k}\right)^{-1} \tag{50}$$

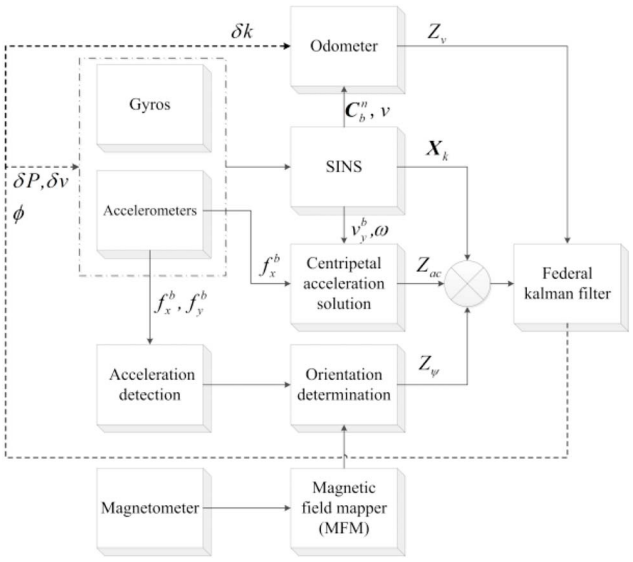

Figure 6. SINS/OD/MAG integrated navigation system.

$$P_{i,k} = \left(I - K_{i,k}H_{i,k}\right)P_{i,k/k-1}\left(I - K_{i,k}H_{i,k}\right)^T + K_{i,k}R_{i,k}K_{i,k}^T \quad (51)$$

Because the main filter has no measurement, there is no measurement update of the main filter.

In the above equations, β_i is the information distribution coefficient, which is determined by the information sharing principle. In the sub-filter, a low accuracy implies a large distribution coefficient of the inertial navigation information. To make the total inertial navigation information to be completely effective in a lower precision subsystem, the accuracy of the subsystem should be high so that β_i is small. Considering the impact of the vehicle road environment and magnetic field factors, the value of β_i can be adapted according to the eigenvalues of covariance matrix *P*. According to Figure 7, synthesized global estimate $\hat{X}_g$ and corresponding covariance matrix P_g of each sub-filter are amplified to $\beta_i^{-1}P_g$ ($\beta_i \le 1$) and fed back to the local filter to reset the estimation of the local filters, i.e.

$$\hat{X}_i = \hat{X}_g \quad (52)$$

$$P_i = \beta_i^{-1}P_g \quad (53)$$

Information fusion is the core step of the federated Kalman filter algorithm. In this integrated navigation system, the locally optimal estimate of each local filter is fused to obtain the globally optimal estimate. The fusion method can be expressed as

$$P_g = \left[P_1^{-1} + P_2^{-1}\right]^{-1} \quad (54)$$

$$\hat{X}_g = P_g\left[P_1^{-1}\hat{X}_1 + P_2^{-1}\hat{X}_2\right] \quad (55)$$

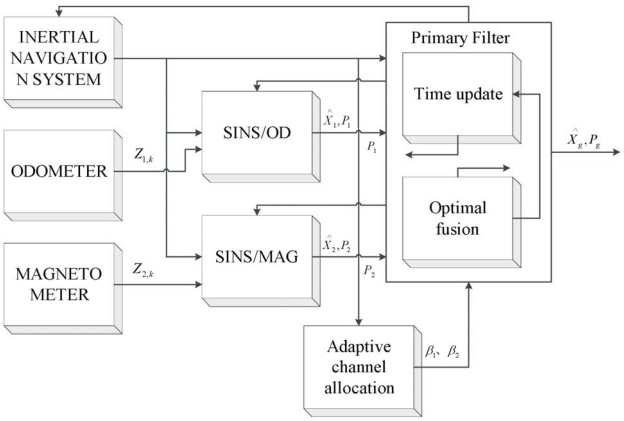

Figure 7. Flow chart of the federated Kalman filter algorithm.

5. Experimental Validation of the Proposed Approach

5.1 Description of the Experiment Platform

To verify the proposed approach, a series of measurements was setup. We used a Xsens MTi-30 sensor and VECTOR CAN bus test equipment to obtain the measurements. The MTi-30 is an attitude heading reference system with an internal integrated tri-axial accelerometer, a tri-axial gyroscope, and a tri-axial MAG sensor. Moreover, the Vector bus test equipment includes CANoe, CANcope, and CANStreessDR, and it can obtain the data from all types of vehicle sensors such as the steering wheel angle sensor and the velocity of the vehicle.

The MTi-30 can output the original data of the accelerometer and gyroscope and filtered attitude information. The MTi-30 specifications are listed in Table 1. The MTi-30 determines the vehicle attitude using an accelerometer, a gyroscope, and a MAG, and removes the magnetic interference of the vehicle before performing the attitude measurement. The installation of the MTi-30 sensor and VECTOR CAN bus test equipment and other devices is shown in Figure 8.

The MTi sensor and CANoe are connected to the same computer by a USB. The corresponding PC software programs are MT Manager and Vector CANape, respectively. The wheel speed sensor is mounted on the front wheel, and its final output data are the average of the right and left wheel speed.

5.2 Tests Performed

The trajectory which was used in the vehicle experi-

Table 1. MTi-30 specifications

	Gyroscopes	Accelerometers	Magnetometer
In-run bias stability	18 °/h	40 μg	--
Noise density	0.03 °/s/√Hz	80 μg/√Hz	200 μg /√Hz
Non-linearity	0.03 %FS	0.03% FS	0.1% FS

ment is presented in Figure 9. During the testing, the total vehicle driving time was 250 s and driving distance was approximately 2 km.

In the measurement process, the sampling frequency of MTi-30 is 100 Hz, wheel speed sensor is 20 Hz, and frequency of the filter update is 20 Hz. The initial latitude and longitude of the experiment were 117.0271° and 36.3612°, respectively, and the initial height was 0 m. To ensure the synchronization of the sensor measurements, the system time was added to the measured data as the time axis. After the experimental testing, the data were outputted to MATLAB for offline simulation.

5.2.1 Experimental Validation of AKF

In the adaptive Kalman filter performance experiment, the attitude, velocity, and position are estimated separately by SINS and SINS/OD that are fused by the AKF. Figure 10 presents the centripetal acceleration $\widetilde{a}_x$ measured by the accelerator of SINS, which is calculated from velocity in the y-axis direction $\widetilde{v}_y^b$ multiplied by z-axis angular velocity $\widetilde{\varphi}$. In this figure, owing to the mutual effect of the vehicle vibration and external impact, the value of $\widetilde{a}_x$ fluctuates around the value of $\widetilde{v}_y^b\widetilde{\varphi}$. In addition, the mean of the centripetal acceleration difference is 0.0021, which is close to 0, so that it can be used as an observation in the SINS/OD system.

The attitude estimation with the Euler angle derived from the MTi-30, SINS, and SINS/OD navigation system fused by AKF, are displayed in Figure 11. It is shown that the attitude derived from the SINS, which is actually calculated by the gyroscopes, suffers from the long-term accumulated errors caused by large sensor biases. Thus, it is necessary to fuse these sensors. By using the AKF, the attitude, velocity, and position error will be implemented to some extent. As can be seen from Figure 11, the attitude calculated output from the proposed SINS/

Figure 8. Experiment platform. ("C" indicates the MTi sensors which are installed on the roof of the vehicle. "D" indicates the computer which collects the data. "E" indicates the VECTOR CAN bus which is connected to the computer.)

Figure 9. Experimental trajectory. ("A" represents the start point and "B" represents the end point.)

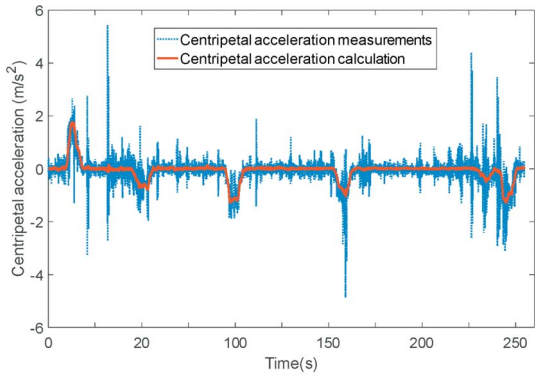

Figure 10. Centripetal acceleration measurements vs. centripetal acceleration calculation in frame *b*.

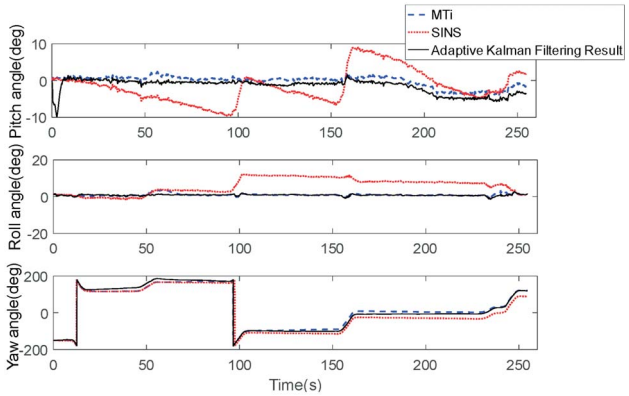

Figure 11. Attitude estimation results of the adaptive Kalman filter.

OD is stable and can track the reference value. It is shown that the mean square error (MSE) [22] of the pitch, roll and, yaw angle (See Table 2 for details) are below 0.35°, 0.28°, and 0.85°, respectively.

To illuminate the effect of the filter, the velocity and position decomposed in the east and north axes are compared with the reference value in Figures 12–14. In Figure 12, it is worth noticing that the MSE between the reference velocity and filtering results are in the east and north directions and less than 0.25 m/s. Moreover, it can be seen that the path estimated by the AKF closely follows the real path and the differences between the reference position and filtering results in the east and north directions are 3.9 m and 4.7 m, respectively in Figure 13 and 14.

This validates the performance of the AKF algorithm implemented in this study. The other test results analysing to validate the performance of the FKF show in next section.

5.2.2 Experimental Validation of FKF

The same path and experiment platform are used to verify the FKF performance, and the attitude estimated separately by SINS and SINS/OD/MAG, which are fused by the FKF, is shown in Figure 15. The figure also shows that the MSE of the pitch, roll, and yaw angle between the reference value and measurement value fused by the FKF are separately 0.45°, 0.25°, and 0.52°.

In this test, the comparison of the velocity and position estimation results between the AKF and FKF are presented in Figures 16–20. Concurrently, Figure 17 is the detailed figure from Figure 16, and it is shown that the velocity estimation results of both the filter methods

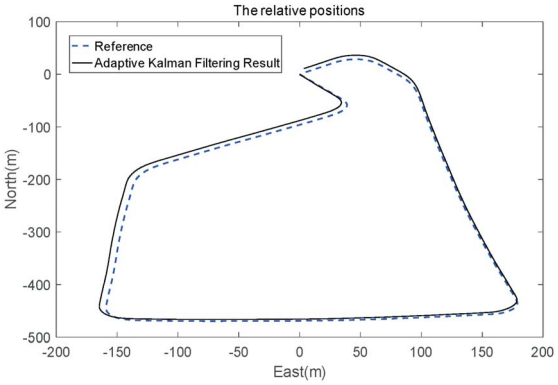

Figure 13. Relative position estimation results of the adaptive Kalman filter.

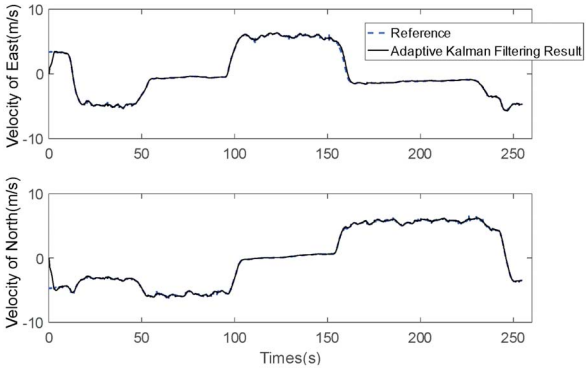

Figure 12. Velocity estimation results of the adaptive Kalman filter.

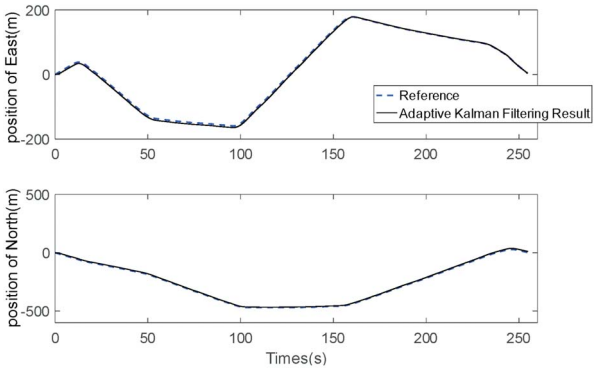

Figure 14. Position estimation results of the adaptive Kalman filter.

Table 2. Estimation error of the integrated navigation

	MSE of AKF results	ME of AKF results	MSE of FKF results	ME of FKF results
Pitch angle (deg)	0.3572	1.6568	0.4587	1.2874
Roll angle (deg)	0.2881	2.2648	0.2584	2.3405
Yaw angle (deg)	0.4466	5.6356	0.5261	5.8210
Velocity of east (m/s)	0.2290	3.4038	0.2070	3.4886
Velocity of north (m/s)	0.2739	4.6958	0.2642	4.7920
Position of east (m)	3.9130	5.5148	4.3570	7.8579
Position of north (m)	4.6986	7.8830	4.4210	8.1630

is in 130–131 s. So is Figure 20, the detail figure from Figure 18, the position estimation results of both the filter methods in 200–201 s is implemented.

From Figures 16 and 19, it can be seen that in the FKF results, the MSE of the velocity in the east and north is 0.2 m/s and 0.26 m/s respectively. The MSE of the position in the east and north are less than 5 meters.

Figures 17 and 20 show the details of the comparison of the AKF and FKF results for the velocity and position with 1 s. It is shown that both the velocity and position estimations made by both the filters are very precisely accurate.

A comparison of the results of AKF and FKF is presented in Table 2. It shows the mean square error (MSE)

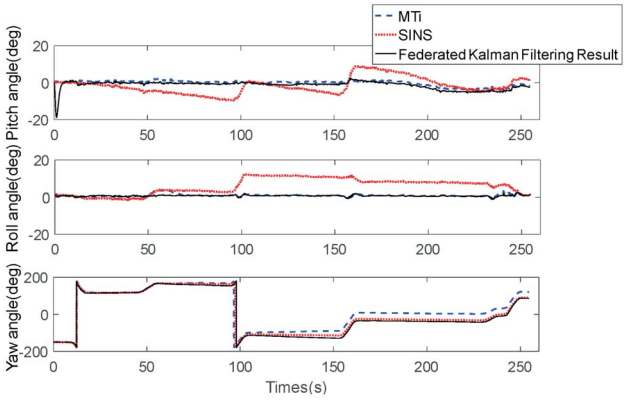

Figure 15. Attitude estimation results of the federated Kalman filter.

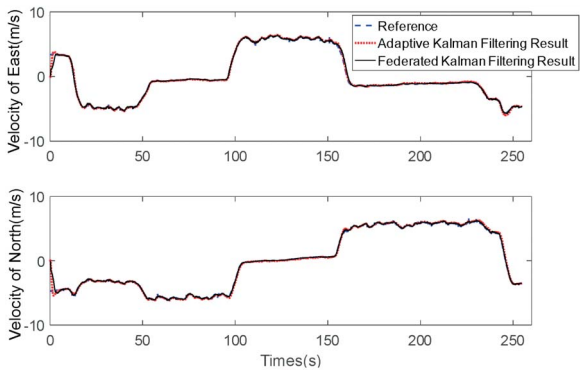

Figure 16. Velocity estimation results of both the filter methods.

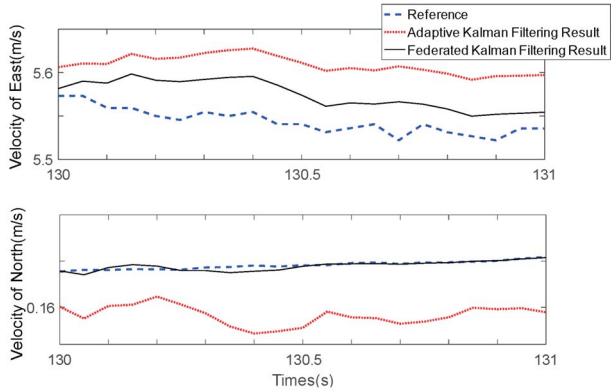

Figure 17. Velocity estimation results of two filter methods in 130–131 s.

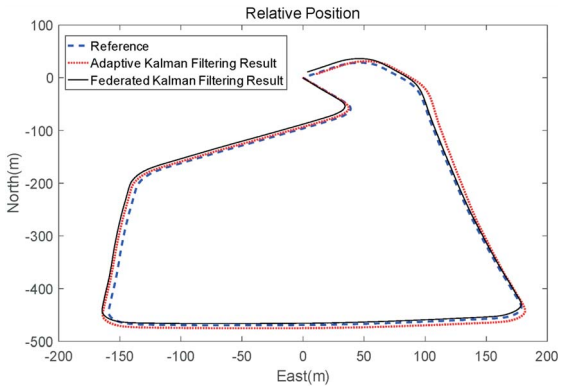

Figure 18. Relative position estimation results of both the filter methods.

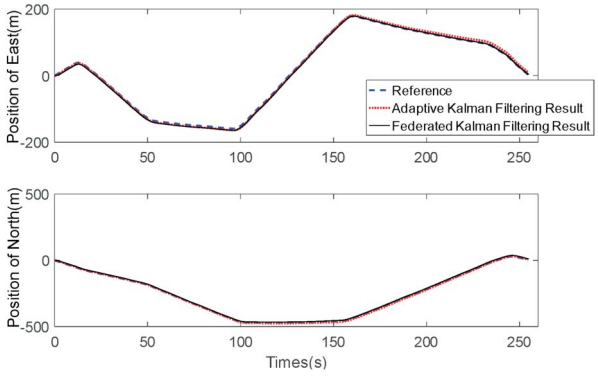

Figure 19. Position estimation results of both the filter methods.

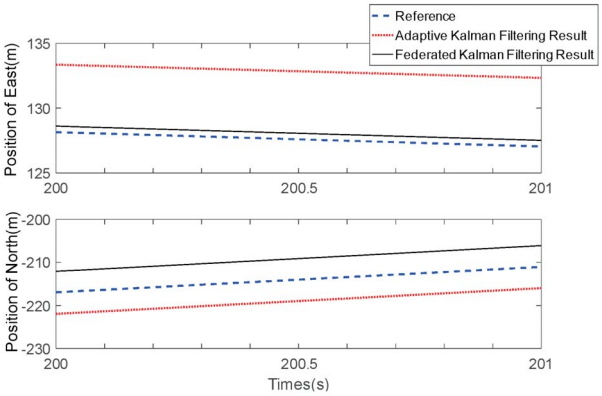

Figure 20. Position estimation results of both the methods in 200–201 s.

and the maximum error (ME) of two filter results. It is clear that the attitude, velocity, and position estimation by both the filters are to have very close. Both the filters can be considered to have satisfactory results. However, the proposed FKF method can not only improve the navigation accuracy in the attitude, velocity, and position, it also promotes the fault-tolerant performance of integrated navigation systems. Then another experiment to test the fault-tolerant performance of FKF is showed in the following sections.

5.3 Fault-tolerant Performance Experiment

To verify the FKF has a good fault-tolerant performance, a comparison testing can be designed. Assuming the case of wheel slipping or locking occurs in 100–110 s, the longitudinal velocity in these abnormal conditions can be shown in Figure 21. When the wheel slipping is in 100–110 s, we assume that the longitudinal velocity which is measured by the wheel speed sensor increases by 20 km/h. Similarly, in the case of wheel locking, the longitudinal velocity measured by the wheel speed sensor is 0 m/s in 100–110 s.

In this experiment, Figures 22 and 23 show the velocity estimation of both the filters when wheel slipping and locking occur in 100–110 s. As shown in the figure, the abnormal conditions of the wheel velocity can generate a large error in the adaptive Kalman filtering result, and it takes a long time to return to the normal condition. This type of system has weak fault isolation and recovery capabilities. However, the FKF uses the principle of information distribution to fuse the SINS/OD and SINS/MAG local systems. The errors caused by the abnormal conditions can be well isolated. When an abnormal situation occurs, the vehicle velocity is actually obtained from the acceleration integral, and the error originates from the integral error acceleration in this time. Therefore, as is shown in Figures 22 and 23, when the wheel slips or locks up, FKF algorithm can well isolate the fault and return to the correct estimated result in a shorter time.

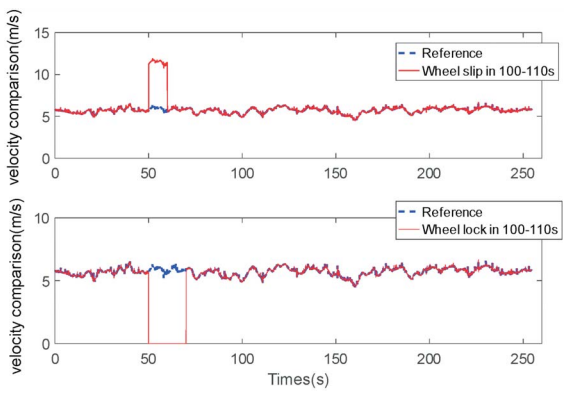

Figure 21. Longitudinal velocity under abnormal conditions.

Thus, test validates that the proposed FKF algorithm provides a high-accuracy velocity estimate and good fault-tolerant performance under abnormal conditions during wheel slipping or locking.

6. Conclusion

In this paper, a new SINS/OD/MAG integrated navigation system is proposed for promoting the accuracy of the attitude, velocity, and position estimation of land vehicle navigation. First, the innovation-based estimation adaptive (IAE) Kalman filter was designed to fuse SINS sensors and odometer measurements, choosing the error of the centripetal acceleration difference as a new obser-

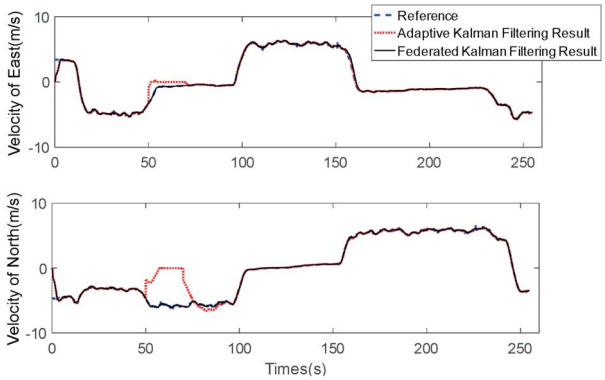

Figure 22. Velocity estimation when the wheel slip is in 100–110 s.

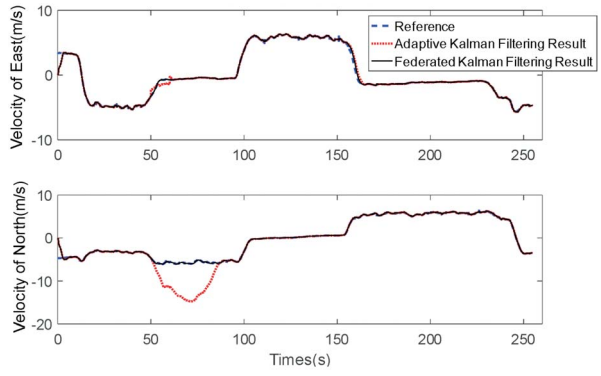

Figure 23. Velocity estimation when the wheel lock is in 100–110 s.

vable in this solution. As we all know, it is difficult to find the accurate noise density without precise knowledge of the model and noise characteristics, because the actual circumstances may be complex and beyond prediction. In conventional Kalman filter, the measurement noise covariance matrix and process noise covariance matrix are fixed and known for priori. Therefore we have applied the adaptive Kalman filter to tune the measurement noise covariance automatically. Then, an adaptive federated Kalman Filter (AFKF) was designed, which integrates a magnetometer based on the SINS/odometer navigation system. This proposed algorithm fused the SINS/OD and SINS/MAG local systems, which can provide high-accuracy navigation information. The federated Kalman filter method that proposed in this paper has the advantages of high accuracy and small amount of communication data, which facility the rapid execution of the algorithm. Compared with the innovation-based estimation adaptive Kalman filter, although both the filters are very precisely. The proposed FKF method can not only improve the navigation accuracy in the attitude, velocity, and position, it can also promote fault-tolerant performance when the odometer measurement was made under abnormal conditions.

Conflict of Interest

The authors declare that there is no conflict of interest regarding the publication of this paper.

References

[1] Titterton, D., J. L. Weston, and J. Weston (2004) *Strapdown Inertial Navigation Technology* 17, IET.

[2] Cai, C. L., L. Yi, and Y. W. Liu (2009) Status quo and trend of inertial integrated navigation system based on MEMS, *Journal of Chinese Inertial Technology* 17, 562–567.

[3] Yu, G.-M., J. Xiong, H. Guo, and J.-X. Wang (2014) GNSS/INS/VKM vehicle integrated navigation system, China Satellite Navigation Conference (CSNC), 2014 Proceedings: Volume III, 585–594. doi: 10.1007/978-3-642-54740-9_51

[4] Morgado, M., P. Batista, P. Oliveira, and C. Silvestre (2011) Position USBL/DVL sensor-based navigation filter in the presence of unknown ocean currents, *Automatica* 47(12), 2604–2614. doi: 10.1016/j.automatica.2011.09.024

[5] Zhou, B., and X. Cheng (2010) Federated filtering algorithm based on fuzzy adaptive UKF for marine SINS/GPS/DVL integrated system, Chinese Control and Decision Conference, 2082–2085. doi: 10.1109/CCDC.2010.5498869

[6] Peng, D., and X. Nie (2009) The low cost MINS/GPS integrated navigation system's design and application, *Chinese Journal of Sensors & Actuators*.

[7] Li, X., and Q. Xu (2016) A reliable fusion positioning strategy for land vehicles in GPS-denied environments based on low-cost sensors, *IEEE Transactions on Industrial Electronics* PP, 1–1.

[8] Wang, M., and Y. Fu (2009) Data fusion of ALV GPS/DR integrated navigation system based on BP neural network, IEEE International Conference on Industrial Technology, 1–4. doi: 10.1109/ICIT.2009.4939595

[9] Cai, C. L., Y. Liu, and Y. W. Liu (2009) Status quo and trend of inertial integrated navigation system based on MEMS, *Journal of Chinese Inertial Technology* 17, 562–567.

[10] Liu, H., Z. Wang, S. Fang, and C. Li (2017) MEMS based SINS/OD filter for land vehicles' applications, *Mathematical Problems in Engineering* 2017, 1–9. doi: 10.1155/2017/1691320

[11] Castagnetti, C., L. Biagi, and A. Capra (2011) Design of a low-cost GPS/magnetometer system for land-based navigation: integration and autocalibration algorithms, In FIG Working Week 2011-Bridging the Gap between Cultures, 1–15.

[12] Thompson, M. J., M. Li, and D. A. Horsley (2011) Low power 3-axis Lorentz force navigation magnetometer, IEEE International Conference on MICRO Electro Mechanical Systems, 593–596. doi: 10.1109/MEMSYS.2011.5734494

[13] Liu, C. S. (2012) A globally optimal iterative algorithm to solve an ill-posed linear system, *Computer Modeling in Engineering & Sciences* 84, 383–403.

[14] Bonnabel, S., P. Martin, and E. Salaun (2009) Invariant extended Kalman filter: theory and application to a velocity-aided attitude estimation problem, Decision and Control, 2009 Held Jointly with the 2009 Chinese Control Conference. Cdc/ccc 2009. Proceedings of the

IEEE Conference on, 1297–1304.

[15] Hemerly, E. M., and V. R. Schad (2005) Real-time implementation of a low cost INS/GPS Kalman filter based navigation system, International Congress of Mechanical Engineering, Ouro Preto.

[16] Bo-Wen, L. I., D. Y. Yao, D. O. Automation, and T. University (2014) Low-cost MEMS IMU navigation positioning method for land vehicle, *Journal of Chinese Inertial Technology*.

[17] Wu, Y., C. Goodall, and N. El-Sheimy (2010) Self-calibration for IMU/odometer land navigation: simulation and test results, In Proceedings of the ION International Technical Meeting, San Diego, CA, USA, 329–334.

[18] Nassar, S., and N. El-Sheimy (2006) A combined algorithm of improving INS error modeling and sensor measurements for accurate INS/GPS navigation, *Gps Solutions* 10(1), 29–39. doi: 10.1007/s10291-005-0149-3

[19] Dah-Jing, J. and T. P. Weng (2008) An adaptive sensor fusion method with applications in integrated navigation, *Journal of Navigation* 61(4), 705–721. doi: 10.1017/S0373463308004827

[20] Loebis, D., R. Sutton, J. Chudley, and W. Naeem (2004) Adaptive tuning of a Kalman filter via fuzzy logic for an intelligent AUV navigation system, *Control Engineering Practice* 12(12), 1531–1539. doi: 10.1016/j.conengprac.2003.11.008

[21] Sokolovic, V. S., G. Dikic, and R. Stancic (2013) Integration of INS, GPS, magnetometer and barometer for improving accuracy navigation of the vehicle, *Defence Science Journal* 63, 451–455. doi: 10.14429/dsj.63.4534

[22] Coco, S., G. Chisari, P. D. Falco, E. Iraci, S. Militello, and A. Laudani (2014) Accurate estimation of vehicle attitude for satellite tracking in Ka Band SOTM, European Modelling Symposium, 409–414. doi: 10.1109/EMS.2014.57

Manuscript Received: Apr. 9, 2018
Accepted: Dec. 7, 2018

Charge Policy

To help defray the rising cost of publication and improve the quality of JASE, some page charge is required for publishing accepted papers.

- The first 8 proof pages including figures, tables and others are charged at US$100 or NTD$3000 for each paper which was accepted after June 1, 2018. Two hardcopies of JASE and the PDF file will be respectively sent to the corresponding author after the official publication.
- For the subsequent pages after eight, the authors will be charged at US $65/per page or NTD $2000/per page.